14th IEA Heat Pump Conference
15-18 May 2023, Chicago, Illinois

Optimum Capacity-Matching Performance of a Heat-Pump-driven Liquid-Desiccant Air-conditioning System

Jae-Hee Lee [a], Yong-Kwon Kang[a], Seheon Kim [a], Gyu-Bae Lee [a], Jae-Weon Jeong [a,*]

[a]Department of Architectural Engineering, College of Engineering, Hanyang University,
222 Wangsimni-Ro, Seongdong-Gu, Seoul, 04763, Republic of Korea

Abstract

In heat-pump-driven liquid-desiccant (HPLD) air-conditioning systems, the release of condensing heat from the heat pump to the regenerator solution and exhaust air (i.e., capacity matching) is very important to maintain the dehumidification performance as well as the operational feasibility and stability of the system. Therefore, in this study, the capacity matching especially focusing on the release of extra condensing heat of the HPLD air-conditioning system is optimized in conjunction with the energy performance. With four design variables under the various outdoor air conditions, a multi-objective optimization is conducted to simultaneously maximize a system coefficient of performance and minimize a newly defined capacity matching index of extra condenser. Pareto front which is a set of optimum points is obtained using multi-objective genetic algorithm, and final optimum solutions are then determined and discussed based on a decision-making scenario. In conclusion, the system coefficient of performance is maximally increased by 24 % and the capacity matching index of extra condenser is maximally decreased by 55 %, compared with each initial value.

Selection and/or peer-review under the responsibility of the organizers of the 14th IEA Heat Pump Conference 2023.

Keywords: Liquid desiccant; Heat pump; Capacity-matching performance; Energy performance; Multi-objective optimization

1. Introduction

Recently, as the significance of indoor humidity control has increased [1], a liquid-desiccant (LD) system which has an energy saving potential due to its decoupled control of the indoor temperature and humidity has emerged as a promising alternative to the traditional dehumidification systems [2]. Both the dehumidification and regeneration performances in the LD system improve via increase of the vapor pressure difference between the desiccant-solution and air. Thus, the desiccant-solution should be cooled before the absorber and heated before the regenerator [3]. Therefore, the integration of a heat pump to the LD system, referred to as a heat-pump-driven liquid-desiccant (HPLD) system, would be a practical approach because the heat pump can provide the solution cooling and heating simultaneously [4].

Many previous studies have mainly focused on improving the energy performance of the HPLD air-conditioning system and demonstrating its energy saving potential [5,6]. By contrast, some previous studies have been performed to match the solution heating load and the actual heat released from the solution-side condenser, and to control the extra condensing load which generates as the heat released from the solution-side condenser is higher than the solution heating load, referred to as capacity matching. Niu et al. [7] defined a novel performance index to evaluate the capacity matching and concluded that the HPLD system should possess double-condenser to handle the extra condensing load. Abdel-Salam and Simonson performed the parametric study on both the capacity matching and energy performance with varying the operating parameters and finally revealed the most influential parameter based on a sensitivity analysis [8]. In addition, they established an operating logic under the various capacity matching situations [9].

* Corresponding author. Tel.: +82-2-2220-2370; fax: +82-2-2220-1945.
E-mail address: jjwarc@hanyang.ac.kr

The abovementioned previous studies focused only on the capacity matching of the solution-side condenser; however, to ensure the operational feasibility and stability of the system, the release of the extra condensing heat in the extra condenser based on thermodynamics should also be concretely handled in the capacity matching research. Furthermore, although the capacity matching, including releasing the extra condensing heat, must finally be optimized considering the energy performance together, no related optimization study has been previously conducted. Therefore, in this study, a multi-objective optimization of the HPLD air-conditioning system which can provide both the latent and sensible cooling is presented. With four design variables under the various outdoor air conditions, the two objectives are optimized as follows: extra condenser's capacity matching index (CMI) which is much focused on releasing the extra condensing heat and coefficient of performance (COP) of the entire system for the energy performance index. A parametric study is first conducted to help to select the design variables and also understand the results of multi-objective optimization. Subsequently, a set of optimum points (i.e., Pareto front) is obtained using multi-objective genetic algorithm (MOGA). This would significantly contribute to providing engineers with a guideline for optimally designing and operating the HPLD air-conditioning system in various situations.

2. System Overview

2.1. System description

Figure 1 shows the proposed HPLD air-conditioning system. The process air as the room-return air mixed with outdoor air is initially dehumidified in the absorber via contact with the desiccant-solution which is cooled to the target temperature by the solution-side evaporator of heat pump. The dried process air is then sensible cooled to the target supply air temperature (i.e., $T_{sa} = 15$ °C) in the air-side evaporator of heat pump. In the regenerator, the desiccant-solution which is heated to the target temperature by the solution-side condenser of heat pump discharges moisture to the outdoor air (i.e., scavenging air) to increase its concentration (i.e., regeneration process). When the amount of heat released from the solution-side condenser is greater than the solution heating load, the extra condenser which is a kind of the air-cooled condenser is activated to release the extra condensing heat into the regenerator outlet air.

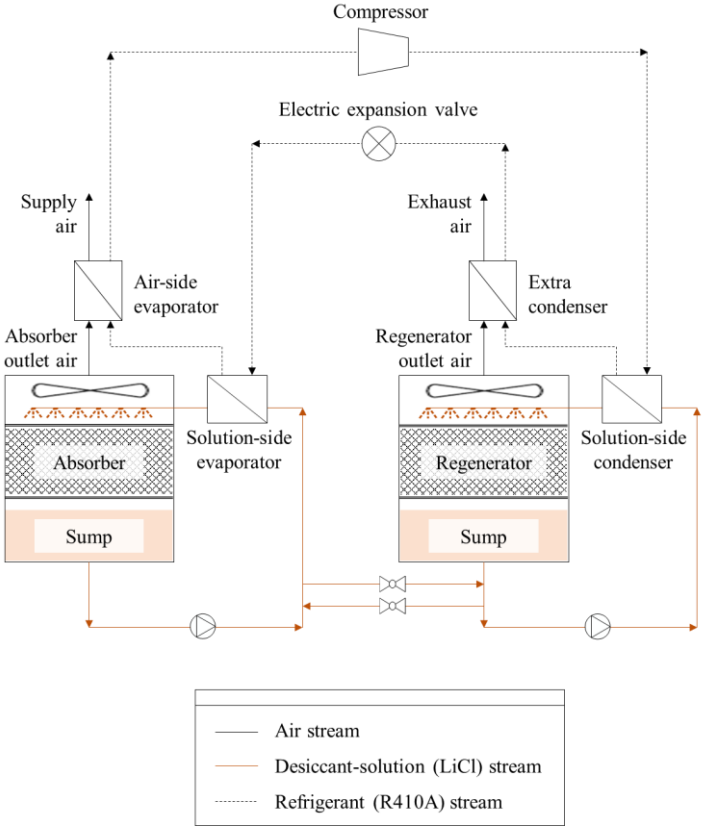

Fig. 1. Proposed HPLD air-conditioning system.

2.2. Performance indices

Before defining the CMI, the amount of heat absorbed by both the solution-side evaporator and air-side evaporator is assumed to be equal to the amount of heat required to cool the absorber solution and process air, respectively. In other words, the actual cooling capacity of evaporator is always the same as the cooling load of evaporator by adjusting the refrigerant flow rate in accordance with the inverter control. Therefore, two evaporators' CMIs (i.e., the ratio of the actual cooling capacity of evaporator to the cooling load of evaporator) are 1.0 all the time, which is not the focus and will not be more discussed in this study. The CMIs of both the solution-side condenser and particularly the extra condenser are the major performance indices to assess the condensing heat release and quantify the capacity matching. The solution-side condenser's CMI ($CMI_{sol,cond}$) is defined as the ratio of the total condensing heat to be released, referred to as total condensing load ($\dot{Q}_{tot,cond,load}$), to the heat required to heating the regenerator solution to the target solution temperature ($\dot{Q}_{reg,load}$) (Eq. (1)).

$$CMI_{sol,cond} = \frac{\dot{Q}_{tot,cond,load}}{\dot{Q}_{reg,load}} = \frac{\dot{m}_{ref}\cdot(h_{cond,i}-h_{cond,o})}{(\dot{m}\cdot c_p)_{reg,i,s}\cdot(T_{reg,i,s}-T_{reg,sump})} \quad (1)$$

Therefore, the increase in $CMI_{sol,cond}$ indicates the increase in the total condensing load, and when $CMI_{sol,cond}$ is greater than 1.0, the extra condensing load ($\dot{Q}_{extra,cond,load}$) then occurs. The extra condenser is a kind of the air-cooled heat exchanger; therefore, the maximum thermodynamically possible heat transfer rate of the extra condenser ($\dot{Q}_{extra,cond,max}$) should be estimated via multiplication of the minimum capacitance rate by the maximum possible temperature difference [10]. Accordingly, the extra condenser's CMI ($CMI_{extra,cond}$) is defined as the ratio of $\dot{Q}_{extra,cond,load}$ to $\dot{Q}_{extra,cond,max}$ (Eq. (2)) to assess the operating stability and feasibility of the extra condenser based on thermodynamics. The decrease in $CMI_{extra,cond}$ indicates the decrease in the extra condensing load, which is ideal in terms of reducing the waste heat and extra condenser size. In addition, when $CMI_{extra,cond}$ is lower than 1.0, the extra condensing heat is well released at the extra condenser. On the other hand, when $CMI_{extra,cond}$ is higher than 1.0, the extra condensing heat is not completely released and remains inside the heat pump, which results in a fatal entire system failure.

$$CMI_{extra,cond} = \frac{\dot{Q}_{extra,cond,load}}{\dot{Q}_{extra,cond,max}} = \frac{\dot{Q}_{tot,cond,load}-\dot{Q}_{reg,load}}{(\dot{m}\cdot c_p)_{reg,o,a}\cdot(T_{cond}-T_{reg,o,a})} \quad (2)$$

The system COP (COP_{sys}) is selected as the energy performance index and defined as the ratio of total cooling capacity ($\dot{Q}_{cooling}$) to total input power ($\dot{W}_{tot}$), as shown in Eq. (3).

$$COP_{sys} = \frac{\dot{Q}_{cooling}}{\dot{W}_{tot}} = \frac{\dot{m}_{abs,i,a}\cdot(h_{abs,i,a}-h_{sa})}{\dot{W}_{comp}+\dot{W}_{fan}+\dot{W}_{pump}} \quad (3)$$

3. Optimization Overview

3.1. Design problem formulation

In the design and operation of the proposed HPLD air-conditioning system, the design problem of multi-objective optimization is formulated to derive the optimum combination of design variables both to achieve the capacity matching including the release of extra condensing heat and to improve the energy performance. The overall design problem formulation is outlined in Table 1.

3.1.1. Design variables

The influential design variables commonly used in the previous studies on the LD systems are as follows: inlet air temperature, inlet air humidity, packing geometry, air flow rate of absorber and regenerator, solution flow rate of absorber and regenerator, solution temperatures of absorber and regenerator, solution concentrations of absorber and regenerator. However, in this study, some of the conventional influential design variables which meet the following criteria are fixed, excluded, or neglected:

- First, the relatively less influential variables
- Second, the uncontrollable or nonmanipulable variables
- Third, the variables related to the latent cooling for a target conditioned zone

Based on the criterion assessment, the multi-objective optimization is conducted for three cases of summer outdoor air temperatures (i.e., low temperature, standard temperature and high temperature), and finally four design variables are selected as follows: the ratio of the air flow rate of regenerator to absorber (R_{air}), the ratio of the solution flow rate of regenerator to absorber (R_{sol}), the solution temperature of absorber ($T_{abs,i,s}$) and the solution temperature of regenerator ($T_{reg,i,s}$). The range of design variables is set in consideration of the range commonly used in the previous studies of the HPLD systems [11] and also the system practicality. Then, the medium of each variable's min-max range was considered as the representative value for each variable and put as its initial value.

3.1.2. Objective function and constraint

Among the performance indices, COP_{sys} and $CMI_{extra,cond}$ are selected as the objective functions to be maximized and minimized, respectively. They also correspond to the constraints because they should be improved compared with their initial values. Particularly, $CMI_{extra,cond}$ must be lower than 1.0 to completely release the extra condensing heat within $\dot{Q}_{extra,cond,max}$, as specified in Section 2.2. In addition, $CMI_{sol,cond}$ corresponds to the constraint too and should be greater than 1.0 because $\dot{Q}_{reg,load}$ should be satisfied to heat the regenerator solution to the target temperature. The humidity ratio of the absorber outlet air ($\omega_{abs,o,a}$) is the final constraint which should be lower than 0.010 kg/kg to handle the room latent load of the target zone [12].

Table 1. Design problem formulation

Category		Parameter	Value
Classification of cases by outdoor air temperature (T_{oa})		Case 1: Low T_{oa} [°C]	$T_{oa} = 27$
		Case 2: Standard T_{oa} [°C]	$T_{oa} = 31$
		Case 3: High T_{oa} [°C]	$T_{oa} = 35$
Design variable	*Find*	R_{air} [-]	$0.5 \leq R_{air} \leq 1.5$ (Initial value: $R_{air} = 1.0$)
		R_{sol} [-]	$0.5 \leq R_{sol} \leq 1.5$ (Initial value: $R_{sol} = 1.0$)
		$T_{abs,i,s}$ [°C]	$15 \leq T_{abs,i,s} \leq 25$ (Initial value: $T_{abs,i,s} = 20$)
		$T_{reg,i,s}$ [°C]	$40 \leq T_{reg,i,s} \leq 50$ (Initial value: $T_{reg,i,s} = 45$)
Objective function	*To maximize*	COP_{sys} [-]	
	To minimize	$CMI_{extra,cond}$ [-]	
Constraint	*Subject to*	COP_{sys} [-]	$COP_{sys} \geq$ Initial value
		$CMI_{extra,cond}$ [-]	$CMI_{extra,cond} \leq$ Initial value, $CMI_{extra,cond} \leq 1.0$
		$CMI_{sol,cond}$ [-]	$CMI_{sol,cond} \geq 1.0$
		$\omega_{abs,o,a}$ [kg/kg]	$\omega_{abs,o,a} \leq 0.010$

3.2. Optimization algorithm

The optimization algorithm should be appropriately selected according to the type of optimization problems. All four design variables are the continuous variables, and because one of the objective functions and constraints has nonlinearity based on the parametric study which will be described later in Section 4.1, nonlinear programming should be handled. In addition, the multi-objective optimization problem with two conflicting objective functions should be solved, and global optimization results, not local optimization results, should be derived. Therefore, MOGA which is based on the genetic algorithm for the multi-objective optimization problem is selected as the optimization algorithm. MOGA is noted as one of the most popular multi-objective optimization algorithms and can generate a better spread of Pareto front for the multi-objective functions. Particularly, two specialized multi-objective operators, corresponding to crowding distance sorting and non-dominated sorting, are applied to MOGA, which is referred to as a non-dominated sorting genetic algorithm-II (NSGA-II) [13]. The population size is 100, and the crossover rate is 0.9. The mutation rate is 0.25 considering the number of design variables, and the random speed is 100. The maximum number of generations is 250, and the violated constraint limit is 0.003. The multi-objective optimization is conducted using a commercial process integration, automation and optimization (PIAnO) software.

4. Results and Discussion

4.1. Parametric study

To help to understand the selection of design variables and the optimization results, the parametric study is first conducted on the two objective functions (i.e., COP_{sys} and $CMI_{extra,cond}$) by varying all possible operating parameters as follows: outdoor air temperature (T_{oa}), outdoor air humidity ratio (ω_{oa}), the ratio of the air flow rate of regenerator to absorber (R_{air}), the ratio of the solution flow rate of regenerator to absorber (R_{sol}), the solution temperature of absorber ($T_{abs,i,s}$) and the solution temperature of regenerator ($T_{reg,i,s}$).

Figure 2 shows the results of parametric study for each operating parameter. As T_{oa} increases, both COP_{sys} and $CMI_{extra,cond}$ are increased (Fig. 2(a)). The increase in COP_{sys} at the high T_{oa} is attributed to the significant increase in the total cooling capacity ($\dot{Q}_{cooling}$). The increase in the heat absorption rate of evaporators and input power of compressor result in the increase in total condensing load ($\dot{Q}_{tot,cond,load}$) and then extra condensing load ($\dot{Q}_{extra,cond,load}$). However, $\dot{Q}_{extra,cond,max}$ is decreased because the difference in the temperature between the regenerator outlet air and condenser is decreased, which increases $CMI_{extra,cond}$.

On the other hand, in Fig. 2(b), COP_{sys} is slightly decreased as ω_{oa} increases because the increase in $\dot{Q}_{cooling}$ is insignificant. In addition, $CMI_{extra,cond}$ is almost constant regardless of the change in ω_{oa} because ω_{oa} is not directly involved in the parameters that make up $CMI_{extra,cond}$.

In Fig. 2(c), COP_{sys} is slightly increased when R_{air} increases because as regenerator air flow rate increases, it could increase the regeneration performance and solution concentration, which increases the dehumidification performance and $\dot{Q}_{cooling}$. However, because the fan power is increased and also the solution cooling load is increased due to the increase in the exothermic reaction during the dehumidification process, COP_{sys} cannot be increased significantly. Meanwhile, $CMI_{extra,cond}$ is found to be much significantly decreased as R_{air} increases due to the increase in the air flow rate of regenerator and the increase in $\dot{Q}_{extra,cond,max}$ accordingly.

In Fig. 2(d), as R_{sol} increases, COP_{sys} is shown to be decreased mainly due to the increase in the pump input power. However, $CMI_{extra,cond}$ is slightly increased as R_{sol} increases. The higher solution flow rate of regenerator is less influenced by the decrease in solution temperature caused by the endothermic reaction during the regeneration process. Therefore, the solution temperature of regenerator sump is increased, and then the condensing temperature is decreased. Consequently, the difference in the temperature between the condenser and the regenerator outlet air is decreased at the high R_{sol}, which results in the $CMI_{extra,cond}$ increase.

In Fig. 4(e), COP_{sys} is maximized between 15–20 °C of $T_{abs,i,s}$. This is because at the higher $T_{abs,i,s}$, the dehumidification rate is decreased due to the decrease in the vapor pressure difference, and at the lower $T_{abs,i,s}$, the dehumidification rate is also decreased according to the previous absorber model used in this study [14]. Therefore, the dehumidification rate is maximized at the intermediate $T_{abs,i,s}$, which results in COP_{sys} being maximized between 15–20 °C of $T_{abs,i,s}$. Meanwhile, as the dehumidification rate is maximized, the regeneration rate is also maximized between 15–20 °C of $T_{abs,i,s}$. Accordingly, the solution temperature of regenerator sump is minimized due to the decrease in solution temperature caused by the endothermic reaction during the regeneration process. Therefore, between 15–20 °C of $T_{abs,i,s}$, $\dot{Q}_{reg,load}$ is maximized and $\dot{Q}_{extra,cond,load}$ is then minimized, which causes the minimization of $CMI_{extra,cond}$.

In Fig. 4(f), as $T_{reg,i,s}$ increases, both COP_{sys} and $CMI_{extra,cond}$ are noted to be decreased. The decrease in COP_{sys} at the high $T_{reg,i,s}$ is resulted from the high input power of the compressor as the condensing temperature is increased to produce the high $T_{reg,i,s}$. On the other hand, the increase in the condensing temperature at the high $T_{reg,i,s}$ increases the temperature difference between the condenser and the regenerator outlet air, thereby decreasing $CMI_{extra,cond}$.

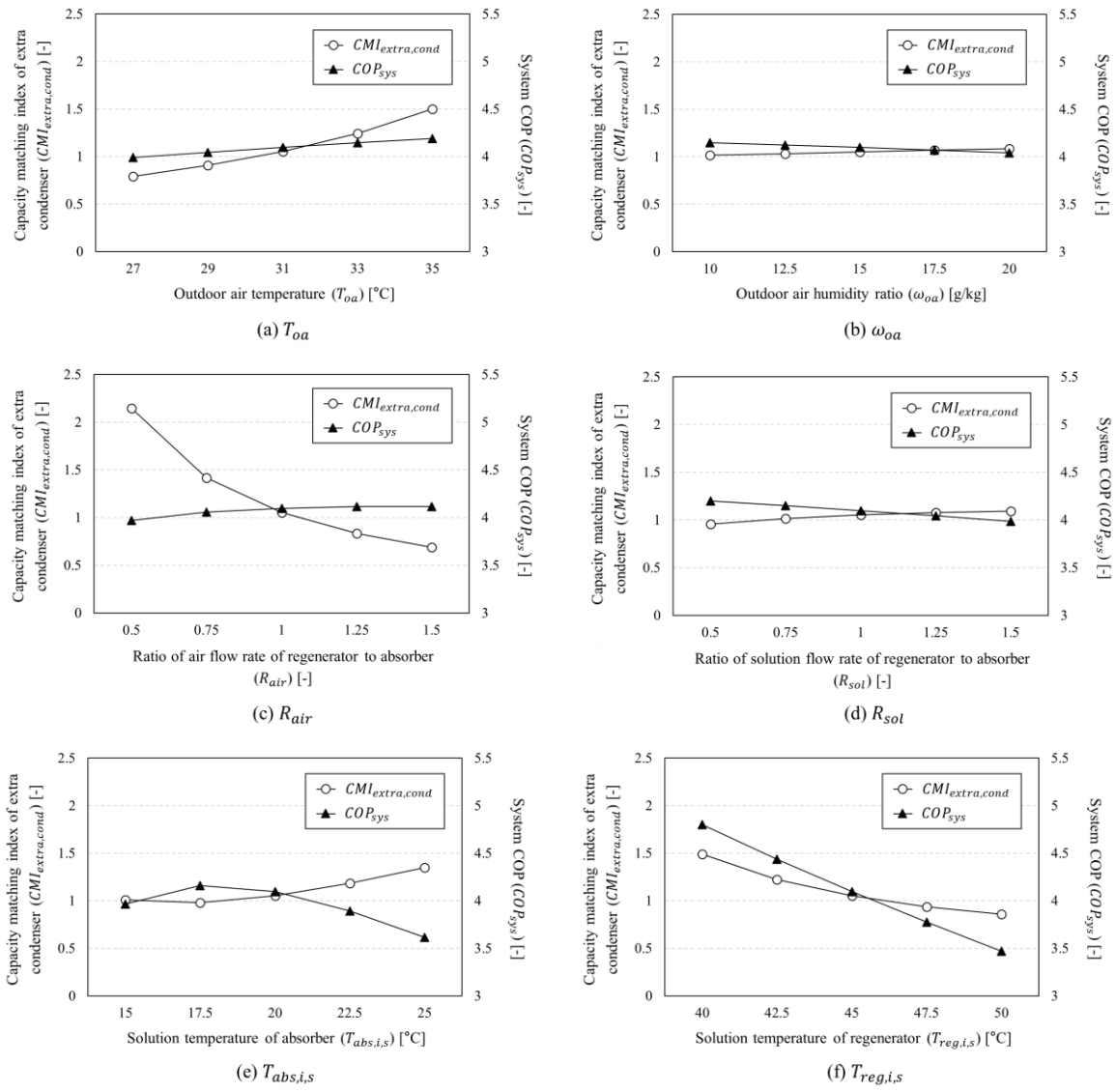

Fig. 2. Effect of operating parameters on two objective functions.

4.2. Optimization results

4.2.1. Pareto front

Pareto front which is a curve presenting a set of optimized non-dominated points obtained by MOGA should be generated to find the optimum solution. Figure 3 shows both the initial model and the generated Pareto fronts by MOGA for each case of T_{oa}. In all three Pareto fronts, all non-dominated optimized points are indicated to be adequately plotted in maximizing COP_{sys} and minimizing $CMI_{extra,cond}$. In addition, the constraints are noted to be satisfied in that all optimized non-dominated points have greater COP_{sys} and lower $CMI_{extra,cond}$ compared to the initial values, respectively, and particularly, all optimized non-dominated points have $CMI_{extra,cond}$ lower than 1.0.

According to the parametric study, when T_{oa} increases, the points of the Pareto front generally have a higher $CMI_{extra,cond}$ value because at the high T_{oa}, releasing the condensing heat is more difficult. Moreover, the maximization of COP_{sys} on the Pareto front in Case 3 is found to be insignificant compared with that in Case 1 and Case 2. This is because in Case 3, in most cases, $CMI_{extra,cond}$ is greater than 1.0 which violates the constraint. Therefore, although COP_{sys} could be further maximized, the points that violate the constraints were excluded from the Pareto front. Meanwhile, in Case 1 and Case 2, a section, names as Section B, is shown on the Pareto front wherein $CMI_{extra,cond}$ is further minimized while COP_{sys} is almost constant. Because R_{air} is the most influential parameter in $CMI_{extra,cond}$, R_{air} is primarily increased in

section B. However, R_{air} is the least influential parameter in COP_{sys}, therefore COP_{sys} is almost constant in Section B. In section A, R_{air} has maximum value and does not change, and then $T_{reg,i,s}$ which corresponds to the next most influential parameter in $CMI_{extra,cond}$ primarily minimizes $CMI_{extra,cond}$. However, $T_{reg,i,s}$ also corresponds to the influential parameter in COP_{sys}, thus the graph rapidly changes in Section A.

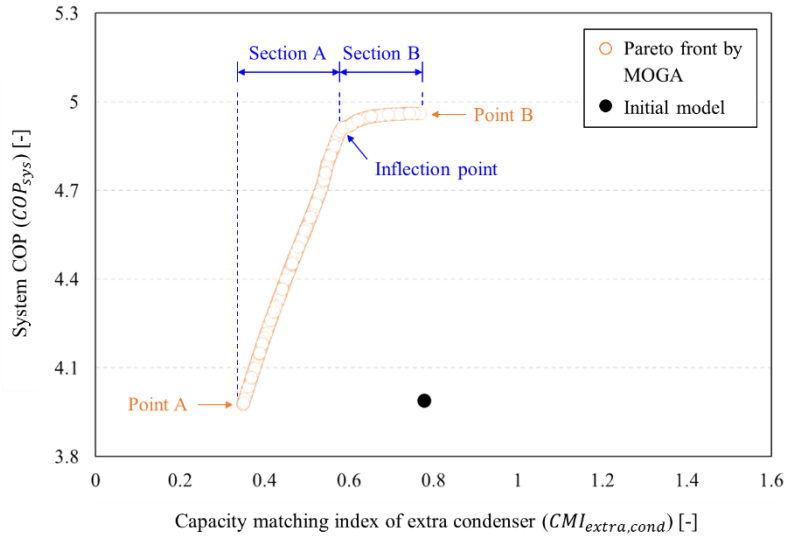

(a) Case 1 ($T_{oa} = 27$ °C).

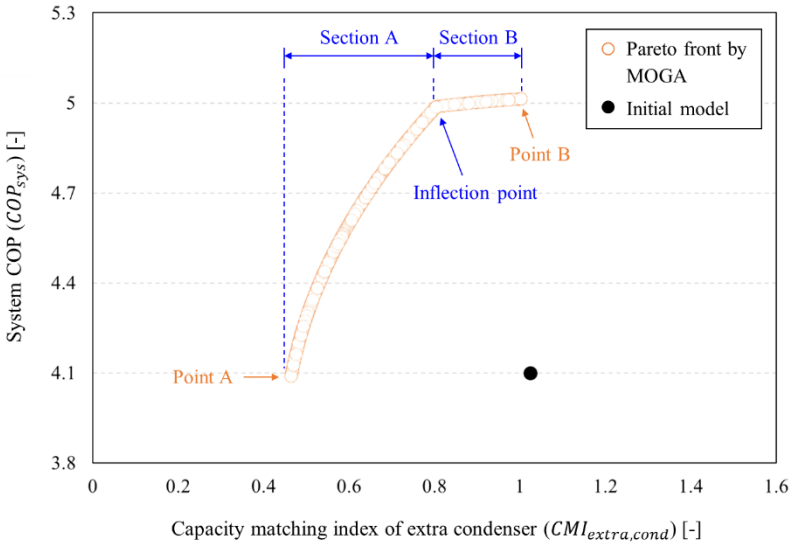

(b) Case 2 ($T_{oa} = 31$ °C).

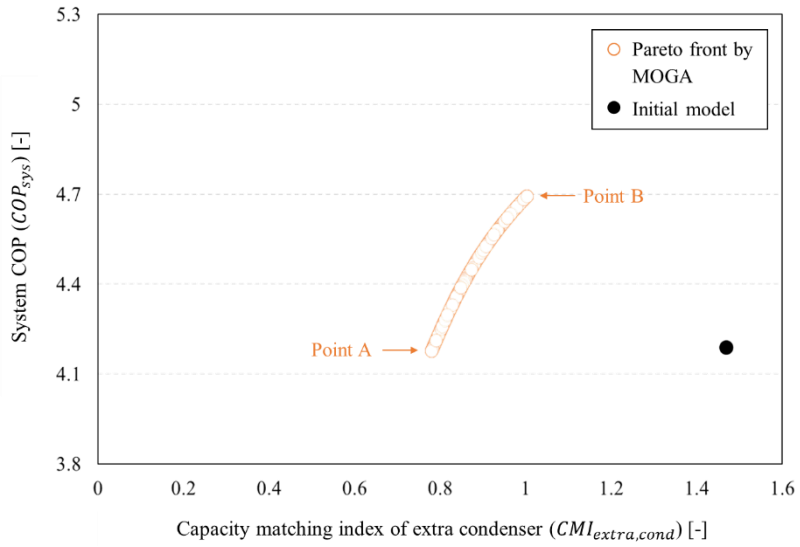

(c) Case 3 (T_{oa} = 35 °C).

Fig. 3. Pareto front generated by MOGA.

4.2.2. Final optimum solutions by decision-making scenario

All non-dominated points on the Pareto front are the acceptable optimum solutions to the multi-objective optimization problem. However, the final optimum solutions should be presented based on a decision-making process to provide the designers and engineers with a practical guideline for optimally designing and operating the HPLD air-conditioning system.

The established decision-making scenario consists of three different scenarios with respect to the different weights allotted to each objective function. First, in Scenario I, COP_{sys} maximization and $CMI_{extra,cond}$ minimization have weights of 0.0 and 1.0, respectively, which corresponds to point A in Fig. 3. Scenario I focuses only on improving the operational feasibility and stability of the system and reducing the extra condensing load while maintaining the energy performance just at its initial value. Second, in Scenario II, COP_{sys} maximization and $CMI_{extra,cond}$ minimization have weights of 0.5 and 0.5, respectively, which places the same importance on both the system energy performance and the heat release. Finally, in Scenario III, COP_{sys} maximization and $CMI_{extra,cond}$ minimization have weights of 1.0 and 0.0, respectively, which corresponds to point B in Fig. 3. Scenario III focuses only on improving the energy performance while maintaining the operational feasibility and stability of the system just at its initial value. Tables 2, 3 and 4 reveal the selected final optimum solutions in all scenarios for each case of T_{oa}.

Table 2. Final optimum solutions based on decision-making scenario for Case 1 (T_{oa} = 27 °C)

Parameter		Decision-making scenario		
		Scenario I	Scenario II	Scenario III
Design variables	R_{air} [-]	1.5	1.5	1.13
	R_{sol} [-]	0.5	0.5	0.5
	$T_{abs,i,s}$ [°C]	15	15	17.3
	$T_{reg,i,s}$ [°C]	46.3	46.3	40.0
Objective functions and Constraints	COP_{sys} [-]	3.99	3.99	4.96
	$CMI_{extra,cond}$ [-]	0.35	0.35	0.77
	$CMI_{sol,cond}$ [-]	1.81	1.81	2.02
	$\omega_{abs,o,a}$ [kg/kg]	0.00798	0.00798	0.00897

Table 3. Final optimum solutions based on decision-making scenario for Case 2 ($T_{oa} = 31$ °C)

Parameter		Decision-making scenario		
		Scenario I	Scenario II	Scenario III
Design variables	R_{air} [-]	1.5	1.5	1.32
	R_{sol} [-]	0.5	0.5	0.5
	$T_{abs,i,s}$ [°C]	18.4	18.2	18.3
	$T_{reg,i,s}$ [°C]	46.3	44.7	40.0
Objective functions and Constraints	COP_{sys} [-]	4.10	4.31	5.01
	$CMI_{extra,cond}$ [-]	0.46	0.51	1.00
	$CMI_{sol,cond}$ [-]	1.93	1.95	2.16
	$\omega_{abs,o,a}$ [kg/kg]	0.00773	0.00800	0.00890

Table 4. Final optimum solutions based on decision-making scenario for Case 3 ($T_{oa} = 35$ °C)

Parameter		Decision-making scenario		
		Scenario I	Scenario II	Scenario III
Design variables	R_{air} [-]	1.5	1.5	1.5
	R_{sol} [-]	0.5	0.5	0.5
	$T_{abs,i,s}$ [°C]	17.0	17.5	18.4
	$T_{reg,i,s}$ [°C]	45.6	44.6	42.4
Objective functions and Constraints	COP_{sys} [-]	4.19	4.35	4.69
	$CMI_{extra,cond}$ [-]	0.78	0.84	1.00
	$CMI_{sol,cond}$ [-]	2.04	2.06	2.15
	$\omega_{abs,o,a}$ [kg/kg]	0.00815	0.00823	0.00849

5. Conclusion

In this study, the multi-objective optimization of the HPLD air-conditioning system was conducted to simultaneously improve the energy performance and achieve the capacity matching especially focusing on the release of extra condensing heat. The capacity matching indices were defined for solution-side condenser and extra condenser, respectively to assess the release of condensing heat and quantify the capacity matching. With four design variables (i.e., R_{air}, R_{sol}, $T_{abs,i,s}$, $T_{reg,i,s}$), a set of optimum points, referred to as Pareto front, which aims maximizing COP_{sys} and minimizing $CMI_{extra,cond}$, was generated based on MOGA for each case of outdoor temperature (T_{oa}). Subsequently, the final optimum solutions were determined based on the decision-making scenario which is established by diversely assigning weights to the objective functions.

Finally, at the low T_{oa}, COP_{sys} and $CMI_{extra,cond}$ maximally increased and decreased by 24 % and 55 %, respectively, compared with initial value, and at the standard T_{oa}, by 22 % and 55 %, respectively, and at the high T_{oa}, by 12 % and 47 %, respectively. The results of this study would be a practical guideline for engineers to optimally design and operate the HPLD air-conditioning system while simultaneously improving the energy performance and capacity matching in various situations. In future, an experimental investigation will be conducted to validate the optimization results in this study, and an optimal prototype will also be constructed based on the optimization results in this study.

Acknowledgements

This work was supported by the National Research Foundation of Korea(NRF) grant funded by the Korea government(MSIT) (No. 2022R1A2B5B02001975 and No. 2022R1A4A1026503) and Korea Environment Industry & Technology Institute (KEITI) through Prospective green technology innovation project, funded by Korea Ministry of Environment (MOE) (RE202103243).

References

[1] Winkler, J., Munk, J., Woods, J. Effect of occupant behavior and air-conditioner controls on humidity in typical and high-efficiency homes. *Energy Build.* 2018;**165**:364–78.
[2] Liu, X., Jiang, Y., Zhang, T. *Temperature and humidity independent control (THIC) of air-conditioning system*. Springer; 2014.
[3] Qi, R., Lu, L., Huang, Y. Energy performance of solar-assisted liquid desiccant air-conditioning system for commercial building in main climate zones. *Energy Convers. Manag*. 2014;**88**:749–57.
[4] Mohammad, A.T., Bin Mat S., Sulaiman, M.Y., Sopian, K., Al-Abidi, A.A. Survey of liquid desiccant dehumidification system based on integrated vapor compression technology for building applications. *Energy Build*. 2013;**62**:1–14.
[5] Cai, D., Qiu, C., Zhang, J., Liu, Y., Liang, X., He, G. Performance analysis of a novel heat pump type air conditioner coupled with a liquid dehumidification/humidification cycle. *Energy Convers. Manag*. 2017;**148**:1291–305.
[6] Liu, X., Xie, Y., Zhang, T., Chen, L., Cong, L. Experimental investigation of a counter-flow heat pump driven liquid desiccant dehumidification system. *Energy Build.* 2018;**179**:223–38.
[7] Niu, X., Xiao, F., Ma, Z. Investigation on capacity matching in liquid desiccant and heat pump hybrid air-conditioning systems. *Int. J. Refrig*. 2012;**35**:160–70.
[8] Abdel-Salam, A.H., Simonson, C.J. Capacity matching in heat-pump membrane liquid desiccant air conditioning systems. *Int. J. Refrig*. 2014;**48**:166–77.
[9] Abdel-Salam, A.H., Simonson, C.J. Optimal design, sizing and operation of heat-pump liquid desiccant air conditioning systems. *Sci. Technol. Built Environ*. 2020;**26**:161–76.
[10] Mitchell, J.W., Braun, J.E. *Principles of heating, ventilation, and air conditioning in buildings*. John Wiley & Sons; 2012.
[11] Liu, X., Yi, X., Jiang, Y. Mass transfer performance comparison of two commonly used liquid desiccants: LiBr and LiCl aqueous solutions. *Energy Convers. Manag*. 2011;**52**:180–90.
[12] Lee, J.H., Jeong, J.W. Hybrid Heat-Pump-driven Liquid-Desiccant System: Experimental Performance Analysis for Residential Air-conditioning Applications. *Appl. Therm. Eng*. 2021;**195**:117236.
[13] Deb, K., Pratap, A., Agarwal, S., Meyarivan, T. fast and elitist multiobjective genetic algorithm: NSGA-II. *IEEE Trans. Evol. Comput*. 2002;**6**:182–197.
[14] Chung, T.W., Luo, C.M. Vapor pressures of the aqueous desiccants. *J. Chem. Eng. Data*. 1999;**44**:1024–27.